Proceedings of the
International Conference on Mechanical Engineering 2011
(ICME2011) 18-20 December 2011, Dhaka, Bangladesh

ICME11-TH-026

.

UNSTEADY TWO-DIMENSIONAL CONVECTIVE HEAT AND MASS TRANSFER FLOW ALONG A WEDGE WITH THERMOPHORESIS

ATM. M. Rahman[1], M. S. Alam [2], M. K. Chowdhury[3] and M.M. Rahman[3]

[1]Department of Computer Science and Engineering, Dhaka International University, Bangladesh
[2]Department of Mathematics, DUET, Bangladesh
[3]Department of Mathematics, BUET, angladesh,

ABSTRACT

In this paper an unsteady two dimensional convective heat and mass transfer flow along a wedge with thermophoresis has been investigated. The governing time dependent non-linear boundary layer equations are made locally similar by introducing a new similarity transformation. The resulting local similarity equation for unsteady flow has been solved numerically by applying Nachtsheim-Swigert shooting iteration technique along with sixth order Runge-Kutta integration scheme. Numerical results for the velocity, temperature and concentration profiles as well as local skin-friction coefficient, rate of heat and mass transfer and thermophoretic deposition velocity for different values of unsteadiness parameter, pressure gradient parameter, thermophoretic parameter, Schmidt number and concentration ratio are displayed in graphically.

Keywords: Unsteady Wedge Flow, Heat And Mass Transfer, Thermophoreshis.

1. INTRODUCTION

Thermophoresis is a phenomenon, which causes small particles to be driven away from a hot surface and toward a cold one. Small particles, such as dust, when suspended in a gas with a temperature gradient, experience a force in the direction opposite to the temperature gradient. Thermophoresis phenomenon plays an important role in a variety of applications such as the production of ceramic powders in high temperature aerosol flow reactors, and the production of optical fiber performs by the modified chemical vapor deposition (MCVD) process. In the optical fiber process, high deposition levels are desired since the goal is to coat the interior of the tube with particles. On the other hand, in ceramic powder production, low deposition levels are desired as deposits lead to reduced product yield and potential pipe blockage. Thermophoretic deposition of radioactive particles is considered to be one of the important factors causing accidents in nuclear reactors. In light of these applications, Peterson et al. [1] studied two different model approaches for aerosol deposition on wafers and the particle concentration profile above a wafer surface. Sasse et al. [2] analyzed the concept of combining thermophoresis with natural convection flow for the design of a control device for capturing sidestream smoke particles. The approach involved numerical simulations of the competition among advection, diffusion, and thermophoresis within a channel between (a) parallel plates and (b) concentric tubes. Their numerical results showed that the temperature difference between the plates, with the cold wall fixed at ambient temperature, does not have a significant effect on the efficiency of particle removal. Tsai and Liang [3] adopted the numerical solutions for self-similar boundary layer flows to develop a rational correlation for evaluating the effect of thermophoresis on aerosol deposition from laminar flow system. In their model they have used the similarity method to estimate the precipitation rates for dust, soot and mist from the aerosol flow. Selim et al. [4] investigated the effect of surface mass transfer on mixed convection flow past a heated vertical flat permeable plate with thermophoresis. Effects of heat generation or absorption on thermophoretic free convection boundary layer from a vertical flat plate embedded in a porous medium have been investigated by Chamkha et al. [5]. Postelnicu [6] studied the effects of thermophoresis particle deposition in free convection boundary layer from a horizontal flat plate embedded in a porous medium. Duwairi and Damesh [7] analyzed the effects of thermophoresis particle deposition on mixed convection from vertical surfaces embedded in saturated porous medium. Alam et al. [8, 9, 10] studied the effects of thermophoresis on steady two-dimensional hydromagnetic heat and mass transfer flow over an inclined flat plate with various flow conditions. Damesh et al. [11] studied non-similar solutions of magnetohydrodynamic and thermophoresis particle deposition on mixed convection problem in porous media along a vertical surface with variable wall temperature. Recently, Rahman and Postelnicu [12] studied the effects of thermophoresis on the forced convective laminar flow of a viscous incompressible fluid over a rotating disk.

Therefore the objective of the present paper is to investigate the effects of thermophoresis on an unsteady two-dimensional hydrodynamic forced convective heat and mass transfer flow of a viscous incompressible fluid along a heated impermeable wedge. By introducing a new class of similarity transformations proposed by Sattar [13], the governing non-linear partial differential equations are reduced to locally similar ordinary differential equations which are solved numerically by applying shooting method.

2. MATHEMATICAL FORMULATION

We consider an unsteady two-dimensional laminar forced convective hydrodynamic heat and mass transfer flow of a viscous incompressible fluid along a heated impermeable wedge (see Fig. 1) in the presence of thermophoresis. The angle of the wedge is given by $\Omega = \beta\pi$. The flow is assumed to be in the *x*-direction which is taken along direction of the wedge and the *y*-axis normal to it. The surface of the wedge is maintained at a uniform constant temperature T_w and a uniform constant concentration C_w which are higher than the ambient temperature T_∞ and ambient concentration C_∞ respectively.

Then under the usual Boussinesq's and boundary layer approximations, the governing equations describing the conservation of mass, momentum, energy and concentration respectively can be written as follows:

$$\frac{\partial u}{\partial x} + \frac{\partial v}{\partial y} = 0, \qquad (1)$$

$$\frac{\partial u}{\partial t} + u\frac{\partial u}{\partial x} + v\frac{\partial u}{\partial y} = \frac{\partial U}{\partial t} + U\frac{\partial U}{\partial x} + \upsilon\frac{\partial^2 u}{\partial y^2} \qquad (2)$$

$$\frac{\partial T}{\partial t} + u\frac{\partial T}{\partial x} + v\frac{\partial T}{\partial y} = \frac{\lambda_g}{\rho c_p}\frac{\partial^2 T}{\partial y^2}, \qquad (3)$$

$$\frac{\partial C}{\partial t} + u\frac{\partial C}{\partial x} + v\frac{\partial C}{\partial y} = D\frac{\partial^2 C}{\partial y^2} - \frac{\partial}{\partial y}(V_T C) \qquad (4)$$

where *u, v* are the velocity components in the *x* and *y* directions respectively, *t* is the time , υ is the kinematic viscosity, ρ is the density of the fluid. T, T_w and T_∞ are the temperature of the fluid inside the thermal boundary layer, the wedge surface temperature and the fluid temperature in the free stream, respectively, while C, C_w and C_∞ are the corresponding concentration, λ_g is the thermal conductivity of the fluid, c_p is the specific heat at constant pressure, D is the molecular diffusivity of the species concentration and V_T is the thermophoretic velocity which is defined as follows

$$V_T = -\frac{k\upsilon}{T}\frac{\partial T}{\partial y}, \qquad (5)$$

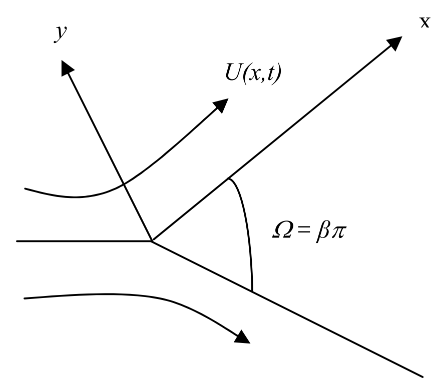

Fig.1. Physical model and co-ordinate system

where k is the thermophoretic coefficient which ranges in value from 0.2 to 1.2 as indicated by Batchelor and Shen [14]

The appropriate boundary conditions for the above model are as follows:

$$u = 0,\ v = 0,\ T = T_w\ ,\ C = C_w\ ,\ \text{at } y = 0 \qquad (6a)$$

$$u = U(x,t), T = T_\infty, C = C_\infty \ \ as \ \ y \to \infty\ , \qquad (6b)$$

where *U(x,t)* is the potential flow velocity for the wedge flow which is taken as follows (see also Sattar [15]):

$$U(x,t) = \frac{\upsilon x^m}{\delta^{m+1}}, \qquad (7)$$

where *m* is an arbitrary constant and is related to the wedge angle and δ is the time dependent length scale which is taken to be (see also Sattar [15,13]) as

$$\delta = \delta\,(t). \qquad (8)$$

In order to obtain similarity solution of the problem we introduce the following non-dimensional variables:

$$\eta = y\sqrt{\frac{(m+1)}{2}}\sqrt{\frac{x^{m-1}}{\delta^{m+1}}},\quad \psi = \sqrt{\frac{2}{m+1}}\,\frac{\upsilon x^{(m+1)/2}}{\delta^{(m+1)/2}}f(\eta),\ \ \theta(\eta) = \frac{T - T_\infty}{T_w - T_\infty}, \phi(\eta) = \frac{C - C_\infty}{C_w - C_\infty} \qquad (9)$$

where η is the similarity variable, ψ is the stream function that satisfies the continuity equation (1) and is defined by $u = \partial\psi/\partial y$ and $v = -\partial\psi/\partial x$.

Now using equations (8)-(9) into equations (2)-(4) we obtain the following non linear ordinary differential equations:

$$f''' + ff'' + \beta(1 - f'^2) - \frac{\delta^m}{\upsilon x^{m-1}}\frac{d\delta}{dt}(2 - 2f' - \eta f'') = 0, \qquad (10)$$

$$\theta'' + \Pr f\theta' + \frac{\delta^m}{\upsilon x^{m-1}}\frac{d\delta}{dt}\Pr \eta\theta' = 0, \qquad (11)$$

$$\phi'' + Scf\phi' + \frac{\delta^m}{\upsilon x^{m-1}}\frac{d\delta}{dt}Sc\eta\phi' + \frac{k\ Sc}{N_t + \theta}[(N_c + \phi)\theta'' + \theta'\phi' - (\frac{N_c + \phi}{N_t + \theta})\theta'^2] = 0 \qquad (12)$$

with the transformed boundary conditions:

$$f = 0, f' = 0, \theta = 0, \phi = 0 \quad at \quad \eta = 0 \,, \qquad (13a)$$
$$f' = 1, \theta = 0, \phi = 0 \quad as \quad \eta \to \infty \,. \qquad (13b)$$

where $\beta = \frac{2m}{m+1}$ is the wedge angle parameter that corresponds to $\Omega = \beta\pi$ for a total angle Ω of the wedge, $\Pr = \frac{\upsilon \rho c_p}{\lambda_g}$ is the Prandtl number, $Sc = \frac{\upsilon}{D}$ is the Schmidt number, $N_t = \frac{T_\infty}{T_w - T_\infty}$ is the thermophoresis parameter, $N_c = \frac{C_\infty}{(C_w - C_\infty)}$ is the concentration ratio.

Now in order to make the equations (10)-(12) locally similar, let

$$\frac{\delta^m}{\upsilon x^{m-1}} \frac{d\delta}{dt} = \lambda, \qquad (14)$$

where λ is taken to be a constant and thus can be treated as a dimensionless measure of the unsteadiness.

Hence equations (10)-(12) becomes

$$f''' + ff'' + \beta(1 - f'^2) - \lambda(2 - 2f' - \eta f'') = 0 \,, \quad (15)$$
$$\theta'' + \Pr f\theta' + \lambda \Pr \eta\theta' = 0 \,, \qquad (16)$$
$$\phi'' + Scf\phi' + \lambda Sc\eta\phi' + \frac{k\ Sc}{N_t + \theta} \qquad (17)$$
$$[(N_c + \phi)\theta'' + \theta'\phi' - (\frac{N_c + \phi}{N_t + \theta})\theta'^2] = 0$$

Further, we suppose that $\lambda = \frac{c}{x^{m-1}}$, where c is a constant so that

$$c = \frac{\delta^m}{\upsilon} \frac{d\delta}{dt} \,. \qquad (18)$$

Thus integrating (18) we obtain that

$$\delta = [c(m+1)\upsilon t]^{1/m+1} \qquad (19)$$

Now taking $c = 2$ and $m = 1$ in equation (19) we obtain $\delta = 2\sqrt{\upsilon t}$ which shows that the parameter δ can be compared with the well established scaling parameter for the unsteady boundary-layer problems [see Schlichting [16].

3. NUMERICAL SOLUTIONS

The set of nonlinear ordinary differential equations (15)-(17) along with the corresponding boundary conditions (13) have been solved numerically by applying sixth order Runge-Kutta integration scheme together with Nachtsheim-Swigert [17] shooting iteration technique [for detailed discussion of the method see also Alam et al.[18]] with β, λ, Pr, Sc, k, N_t and N_c as prescribed parameters. A step size of $\Delta\eta = 0.01$ was selected to be satisfactory for a convergence criterion of 10^{-6} in all cases. The value of η_∞ was found to each iteration loop by the statement $\eta_\infty = \eta_\infty + \Delta\eta$. The maximum value of η_∞ to each group of parameters β, λ, Pr, Sc, k, N_t and N_c determined when the value of the unknown boundary conditions at $\eta = 0$ does not change to successful loop with an error less than 10^{-6}.

4. TESTING OF THE CODE

To check the validity of the present code we have calculated the values of $f''(0)$ for the Falkner-Skan boundary layer equation for the case $\beta = 0$ and $\lambda = 0$ for different values of η. Thus from table-1 we observe that the data produced by the present code and those of White [19] are in excellent agreement. This lends confidence in the present numerical method.

Table 1: Comparison of the present numerical results of Falkner-Skan boundary layer equation for the case of β = 0 and $\lambda = 0$.

η	$f''(\eta)$	
	Present work	White[19]
0.0	0.47027089	0.46960
0.5	0.46568757	0.46503
1.0	0.43494906	0.43438
1.5	0.36218408	0.36180
2.0	0.25581418	0.25567
3.0	0.06763291	0.06771
4.0	0.00684790	0.00687
5.0	0.00025589	0.00026

5. RESULTS AND DISCUSSION

Numerical calculations have been carried out for different values of β, λ, Pr, Sc, k, N_t and N_c. The values of Pr have taken to be 0.71, 1.0, 4.34 and 7.0 which correspond physically to air, electrolyte solution and water at two different temperatures 40^{0}C and 20^{0}C respectively.. The values of Schmidt number Sc are taken for hydrogen $(Sc = 0.22)$, helium $(Sc = 0.30)$, water-vapour $(Sc = 0.60)$ and Carbon-Dioxide $(Sc = 0.94)$. It is also worth to mention that according to the definition of the thermophoresis parameter N_t and concentration ratio parameter N_c always greater than one. The effect of changes in the wedge angle parameter β on the dimensionless velocity function f' against η is displayed in Fig. 2(a) for the values 0, 1/6, 1/2, 1 and 1.6. The value of $\beta = 0$ corresponds to wedge angle of zero degree i. e. flat plate, $\beta = 1/2$ corresponds to the wedge angle of 90 degrees i. e. the vertical plate and $\beta = 1$ corresponds to the wedge angle of 180 degrees i. e. stagnation point flow. From this figure it is clear that as the wedge angle parameter β increases the fluid velocity also increases.

The results also show that the velocity profiles became steeper for larger values of the wedge angle parameter β. The wedge angle parameter is a measure of the pressure gradient, and so a positive value of β indicates a negative (or favorable) pressure gradient. It is also mentionable here that separation is found to occur for very small non-negative values of β.

(a)

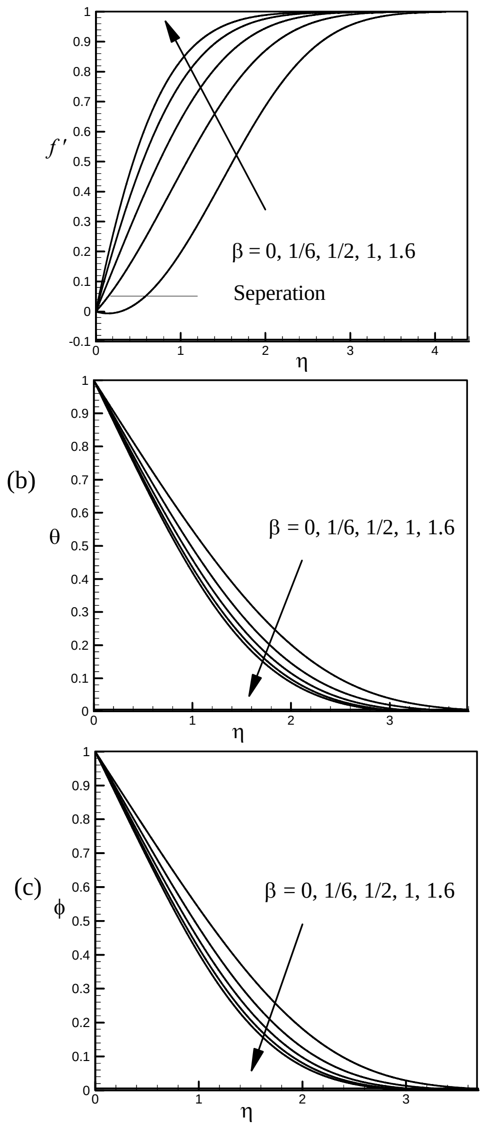

Fig. 2. Dimensionless (a) velocity, (b) temperature and (c) concentration for different values of β while λ = 0.3, Pr = 0.71, Sc = 0.94, Nc = 3.00, k = 0.50 and N_t = 2.00

Physically this means that unlike the case of steady solution obtained by Hartree [20], the unsteady boundary layer is not able to support a small acceleration without separation. Nonetheless, the profiles for the unsteady case follow the same trend of those for the steady case (see Schlichting and Gersten [21]). This result is also consistent with the works of Sattar [13]. Fig. 2 (b) shows non-dimensional temperature profiles within the boundary layer for different values of the wedge angle parameter. From this figure we see that the temperature profiles decrease with the increasing values of the wedge angle parameter β . The effects of the wedge angle parameter on the dimensionless concentration profiles are shown in Fig. 2(c) and we observe that as the wedge angle parameter increases, the concentration profiles decreases.

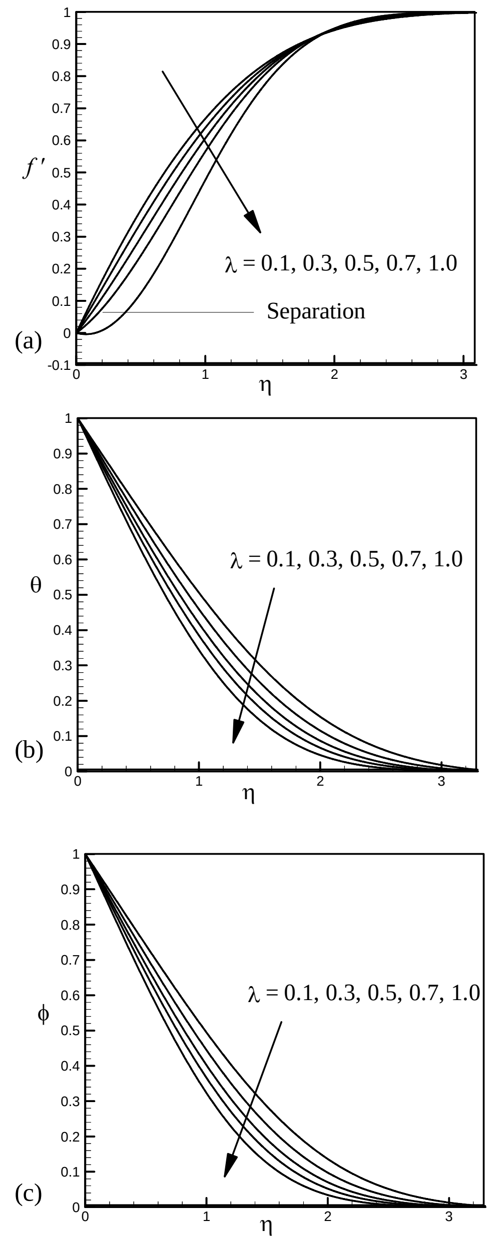

Fig 3. Dimensionless (a) velocity, (b) temperature and (c) concentration for different values of λ while β = 0.5 (i. e. $\Omega = 90^0$), Pr = 0.71, Sc = 0.94, Nc = 3.00, k = 0.50 and N_t = 2.00

The effects of the unsteadiness parameter λ on the dimensionless velocity profiles within the boundary layer are shown in Figs. 3(a) when wedge angle parameter β takes the values 1/2 (vertical plate flow). From these figures we observe that for large values of the parameter λ that is for higher unsteadiness, separation occurs even in the case of accelerated flow or of adverse pressure gradient $(m > 0, \beta > 0)$ which is on the contrary to the findings of Hartree [20] for the steady wedge flow. The effects of the unsteadiness parameter on the non-dimensional temperature and concentration profiles are displayed in 3(b)-3(c), respectively. From these figures we observe that both the temperature and concentration profiles decrease with the increasing values of the unsteadiness parameter λ .

The influence of Prandtl number *Pr* on the temperature profiles within the boundary layer is depicted in Fig.4.

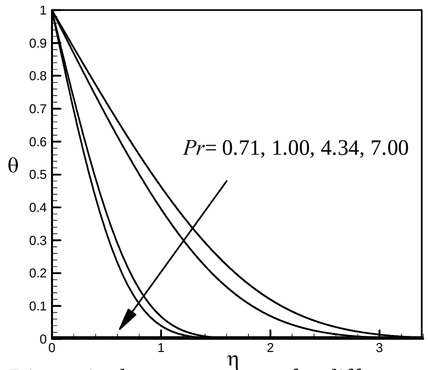

Fig 4. Dimensionless temperature for different values of *Pr* while β = 1/6 (i. e. $\Omega = 30^0$), λ = 0.50, *Sc* = 0.94, *Nc* = 3.00, *k* = 0.50 and N_t = 2.0.

Prandtl number defines the relative effectiveness of the momentum transport by diffusion in the hydrodynamic (velocity) boundary layer to the energy transported by thermal diffusion in the thermal boundary layer. According to the definition of Prandtl number high *Pr* fluids posses lower thermal conductivities which reduces the conduction heat transfer and increases temperature variations at the wall. Low *Pr* fluids have higher thermal conductivities and hence for $Pr < 1$, the thermal boundary layer will be thicker than the velocity boundary layer. Conversely for $Pr > 1$, the thermal boundary layer will be thinner than the velocity boundary layer.

For the special case of $Pr = 1$, the two boundary layer will approximately of equal extent. An increase in *Pr* from 0.71, through 1, 4.34, 7, as shown in Fig. 4, therefore causes a strong decrease in temperature function θ , throughout the flow domain. With larger *Pr* values, thermal diffusivity is much less than the momentum diffusivity causing a decrease in temperature in the boundary layer. In order to examine the effect of thermophoresis on particle deposition onto a wedge surface, the concentration profiles are displayed in Fig. 5 (a), for relative temperature difference parameter N_t . From this figure it is clear that the concentration profiles are decreased when temperature ratios are increased; this is due to small temperature differences between the wedge surface and free stream conditions. The effect of the thermophoretic coefficient k on the concentration profiles are shown in Fig. 5(b). This figure shows that as the thermophoretic coefficient is increased the concentration is also increased; this is due to favorable temperature gradients.

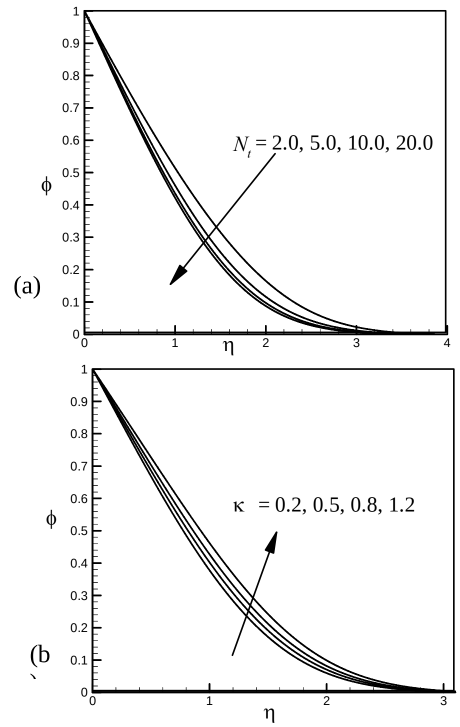

Fig 5. Dimensionless concentration profiles for different values of (a) N_t (*k* = 0.50) and (b) *k* (N_t = 2.0) while β = 1/6 (i. e. $\Omega = 30^0$), *Pr* = 0.71, *Sc* = 0.94, λ = 0.50, *Nc* = 3.00.

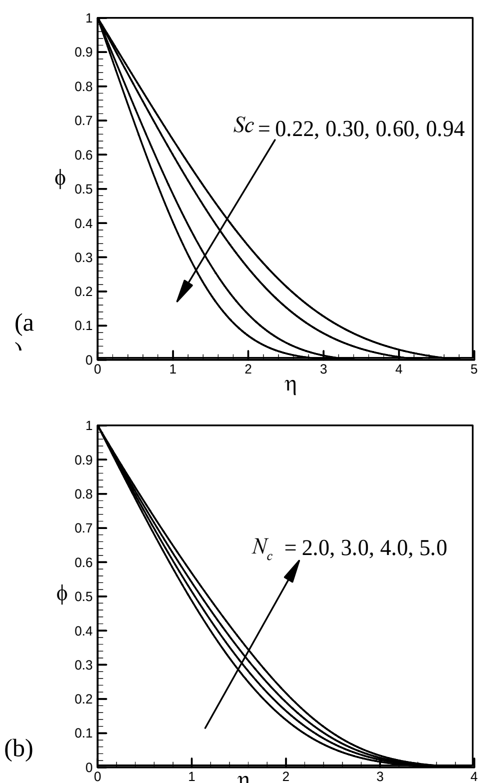

Fig 6. Dimensionless concentration profiles for different values of (a) *Sc* (*Nc* = 0.50) and (b) *Nc* (*Sc* = 0.94) while β = 1/6 (i. e. $\Omega = 30^0$), *Pr* = 0.71, *Sc* = 0.94, λ = 0.50, *k* = 0.50, N_t = 2.0.

Fig. 6 (a) shows the effect of the Schmidt number *Sc* on the dimensionless concentration profiles. We note that the Schmidt number embodies the ratio of the momentum to the mass diffusivity.

Schmidt number therefore quantifies the relative effectiveness of the momentum and mass transport by diffusion in the hydrodynamic (velocity) and concentration (species) boundary layers. From this figure we see that the concentration profiles decrease with the increasing values of *Sc* and this is the analogous to the effect of increasing the Prandtl number on the thickness of the thermal boundary layer. From Fig.6 (b) observe that the concentration ratio profiles increases with the increase of N_c and this due to the favorable concentration difference between the wedge surface and the free stream conditions.

5. CONCLUSIONS

In this paper we have discussed the effects of thermophoresis on an unsteady two-dimensional forced convective heat and mass transfer flow over a heated impermeable wedge. The governing non-linear partial differential equations are transformed into locally similar boundary layer equations which are solved numerically by applying shooting method. Comparisons with previously published work were performed and the results were found to be in excellent agreement. From the present numerical investigations the following major conclusions may be drawn:

i. As the wedge angle parameter increases, the growth of the hydrodynamic, thermal and concentration boundary layers thickness decreases. Separation may occur for small values of. $\beta \geq 0$

ii. Velocity, temperature and concentration profiles decrease as the unsteadiness parameter increases. In the particular case of $\beta = 1/2$ (vertical plate), back flow is found to occur for lower values of $\lambda = 0.7$ which give rise to decelerated flow close to the wall.

6. REFERENCES

1. Peterson T. W., Stratmann F., Fissan H., 1989, Particle deposition a wafers: A comparison between two modeling approaches, J. Aerosol Sci., 20(6) ,483-493.
2. Sasse A. G. B. M., Nazaroff W. W., Gadgil A. J., 1994, Particle filter based on thermophoretic deposition from natural convection, Aerosol Sci. and Tech., 20 ,227-238.
3. Tsai R., Liang L.J., 2001, Correlation for thermophoretic deposition of aerosol particles onto cold plates, J. Aerosol Sci., 32, 473-487.
4. Selim A., Hossain M. A., Rees D.A.S. 2003, The effect of surface mass transfer on mixed convection flow past a heated vertical flat permeable plate with thermophoresis, Int. J. Thermal Sci., 42, 973-982.
5. Chamkha A. J., Al-Mudhaf A. F., Pop I. 2006, Effects of heat generation or absorption on thermophoretic free convection boundary layer from a vertical flat plate embedded in a porous medium, Int. Comm. Heat and Mass Transfer, 33, 1096-1102.
6. Postelnicu A. 2007, Effects of thermophoresis particle deposition in free convection boundary layer from a horizontal flat plate embedded in a porous medium, Int. J. Heat and Mss Transfer, 50, 2981-2985.
7. Duwairi H. M., Damesh R. A. 2008, Effects of thermophoresis particle deposition on mixed convection from vertical surfaces embedded in saturated porous medium, Int. J. Numer. Meth. Heat Fluid Flow, 18(2), 202-216.
8. Alam M. S., Rahman M. M., Sattar M. A. 2008a, Effects of variable suction and thermophoresis on steady MHD combined free-forced convective heat and mass transfer flow over a semi-infinite permeable inclined flat plate in the presence of thermal radiation, Int. J. Thermal Sci., 47, 758-765.
9. Alam M. S., Rahman M. M., Sattar M. A. 2008b, Effects of chemical reaction and thermophoresis on MHD mixed convective heat and mass transfer flow along an inclined plate in the presence of heat generation/absorption with viscous dissipation and joule heating, Can. J. Physics, 86, 1057-1066.
10. Alam M. S., Rahman M. M., Sattar M. A. 2009, On the effectiveness of viscous dissipation and Joule heating on steady Magnetohydrodynamic heat and mass transfer flow over an inclined radiate isothermal permeable surface in the presence of thermophoresis, Comm. in Nonlinear Sci. Numer. simulat., 14, 2132-2143.
11. Damesh R. A., Tahat M. S., Benim Ac. 2009, Non-similar solutions of magnetohydrodynamic and thermophoresis particle deposition on mixed convection problem in porous media along a vertical surface with variable wall temperature, Progress in Comput. Fluid Dynamics, 9(1), 58-65.
12. Rahman M. M., Postelnicu A. 2010, Effects of thermophoresis on the forced convective laminar flow of a viscous incompressible fluid over a rotating disk, Mech. Res. Cumm., 37, 598-603.
13. Sattar M. A. 2011, A local similarity transformation for the unsteady two-dimensional hydrodynamic boundary layer equations of a flow past a wedge, Int. J. Appl. Math. and Mech., 7(1), 15-28.
14. Batchelor G. K., Shen C. 1985, Thermophoretic deposition of particles in gas flowing over cold surface, J. Colloid Interface Sci., 107, 21-37.
15. Sattar M. A. (1994), Unsteady hydromagnetic free convection flow with Hall current, mass transfer and variable suction through a porous medium near an infinite vertical porous plate with constant heat flux, Int. J. Energy Res., 18(9), 771-775.
16. Schlichting H.1968, Boundary layer theory, McGraw Hill.
17. Nachtsheim P. R., Swigert P. 1965, Satisfaction of the asymptotic boundary conditions in numerical solution of the system of non-linear equations of boundary layer type, NASA TND-3004.
18. Alam M. S., Rahman M. M. 2006, Samad M. A., Numerical study of the combined free-forced

convection and mass transfer flow past a vertical porous plate in a porous medium with heat generation and thermal diffusion, Non-linear Analysis: Modelling and Control, 11, 331-343.
19. White F. M. 2006, Viscous Fluid Flows, third ed. McGraw-Hill, New York.
20. Hartree D. R. 1937, On an equation occuring in Falkner and Skan's approximate treatement of the equations of the boundary layer, Proc. Cambr. Phil. Soc., 33, Par II.
21. Schlichting H., Gersten K. 2000, Boundary Layer Theory, 8th Edition, Springer- Verlag, Berlin/Heidelberg.

7. MAILING ADRESS

ATM. M. Rahman
Department of Computer Science and Engineering,
Dhaka International University,
Dhaka-1205, Bangladesh
E-mail: [1]*atmmrahman2005@gmail.com*